

In situ synthesis of fluorescent silicon nanodots for determination of total carbohydrates in a paper microfluidic device combined with laser prepared graphene heater

Inmaculada Ortiz-Gómez ^{a, c}, Víctor Toral-López ^{b, d}, Francisco J Maldonado Romero ^{b, d}, Ignacio de Orbe-Payá ^{a, c}, Antonio García ^b, Noel Rodríguez ^{b, d}, Luís Fermín Capitán-Vallvey ^{a, c}, Diego P Morales ^{b, c, *}, Alfonso Salinas-Castillo ^{a, c, *}

^aECsens, Department of Analytical Chemistry, Faculty of Sciences, 18071 University of Granada, Granada, Spain.

^bResearch Group, Department of Electronics and Computer Technology, Faculty of Sciences, 18071 University of Granada, Spain

^cUnit of Excellence in Chemistry applied to Biomedicine and the Environment, University of Granada, Spain

^dPervasive Electronics Advanced Research Laboratory, University of Granada, 18071 Granada, Spain

*Corresponding author: E-mail address: alfonsos@ugr.es (Alfonso Salinas Castillo) and diegopm@ugr.es (Diego P. Morales)

Abstract

We report a simple, rapid, low-resource and one-step method for formation of fluorescent silicon nanodots (SNDs) in a microfluidic paper-based analytical device (μ PAD) incorporated in a reusable, portable and flexible heater for determination of total carbohydrates. The synthesis of SNDs is based on the redox reaction between (3-aminopropyl) triethoxysilane (APTS) reagent and carbohydrates, which act as a reducer. The graphene-based heater was fabricated by laser ablation of Kapton polyimide. Thereby, the developed system heat the μ PAD during the synthesis of SNDs at 80°C for 30 min. The blue emitting SNDs formed have an emission peak wavelength at 475 nm. We used a digital camera and smartphone for the quantitative analysis of total carbohydrates expressed such as index of glucose or fructose with grey scale value as the analytical parameter. Under the optimal conditions, the method has a low detection limit (0.80 μ M for glucose and 0.51 μ M for fructose, respectively), and a linear

response (10-200 μM for glucose and 10-100 μM for fructose). The method has been applied to the determination of glucose in biological fluids (serum and urine samples). In addition, determination of total carbohydrates in commercial juices and teas has been carried out.

Keywords: Silicon nanodots; Total carbohydrates; Color measurement; μPAD ; Smartphone; Laser Induced Graphene heater; Laser-scribing

1. Introduction

Microfluidic paper-based analytical devices (μPADs) [1] have recently received a huge attention for the design of chemical analysis platforms due to their inherent advantages such as eco-friendly support, manipulation of small volumes of fluids reducing the consumption of samples and reagents, minimization of the complexity of analytical procedures, reduction of the assay time, portability, wearability, lower cost per test, higher sensibility and integration into miniaturized analytical devices, among others [2] [3].

Thereby, microfluidic technologies have been employed in developing point of care (POC) diagnostics [4], [5], [6]. The integration of various emerging functional nanomaterials in μPADs has opened the possibility of expanding their potential. For example, advanced diagnostic technologies, such as POC diagnostics use nanomaterials for optical or electrochemical detection of multiple analytes or markers [7]. Moreover, multiple conventional detection techniques, such as colorimetric detection fluorescence, electrochemical detection, surface-enhanced Raman Spectroscopy have been integrated into μPAD for POCT assays [8],[9], [10],[11], [12].

In this way, semiconductor materials such as silicon, have emerged as a new nanomaterial to construct luminescent probes on the basis of their intrinsic properties: size, shape, composition, surface modification, high luminescence, strong photostability, good biocompatibility and low toxicity [13], [14]. Current research efforts focus on the development of silicon materials for a diverse range of applications, such as batteries, photocatalysis, plasmon enhanced spectroscopy, optical devices,

biological imaging screening and sensors, among others [15]–[18]. In this sense, silicon nanodots (SNDs) have a great potential as novel nanomaterials to fabricate fluorescent probes for sensing. However, studies on SNDs are limited due to their complicated synthesis procedures, strict experimental conditions and use of costly equipment involved in the fabrication [13], [19]–[21]. Different versatile methods have been developed to produce silicon nanodots, for example solution-phase reductive strategy, sonochemical synthesis, microwave irradiation, mechanochemical method, laser ablation, microemulsion, and plasma-assisted aerosol precipitation [22]–[27]. These methodologies require complicated procedures, harsh experiment conditions and costly equipment. For example, microwave method requires high temperature ($\sim 160^\circ\text{C}$), high pressure (~ 10 - 15 times atmospheric pressure) and costly microwave equipment to produce silicon nanoparticles [28].

Thus, simple and eco-friendly synthesis strategies which eliminate or reduce the use of chemical compounds as well as energy exhaustive processes are highly desirable [29]. For all this, the possibility to implement chemical reagent for nanomaterials in microfluidic platforms such as μPAD could minimize these drawbacks, allowing the in situ generation of the SNDs which reduces their aging and so, assures the reliability of the measuring process.

In this direction, flexible electronics are a great allied. New materials as graphene nano-aggregates and nanowires combined with inkjet printing and laser scribing techniques, among others, ease and increase the development of miniaturized flexible devices [30], [31], [32]. One of these devices are flexible film heaters which can be used to accelerate the reaction to generate SNDs [33].

Thus, this work investigates the possibility of combining handheld readers such as smartphone with these devices to control a chemical reaction or process in a microfluidic system that increases their capabilities. Specifically, we present an application of a heater in combination with a smartphone to control a chemical reaction. A flexible Laser Induced Graphene (LIG) heater studied in a previous work [34] is combined with electronic hardware to create a system with communications capabilities that can control the temperature of the reaction. The result of this combination is a cost-effective, reusable system to control the chemical reaction to determine total carbohydrates.

In summary, this work describes a μ PAD for direct determination of total carbohydrates with one-step synthesis of fluorescent SNDs using a reusable, cost-effective, flexible and portable LIG heater. The novelty of the proposed assay is based on the combination of paper-based microfluidic device and a LIG heater, which provides the energy necessary to heat the paper and facilitate the synthesis of SNDs. Thereby, this non-enzymatic method for the determination of total carbohydrates is based on the possibility to relate the increase of fluorescence intensity of SNDs with the concentration of carbohydrates in a sample. Therefore, the measurement of glucose and fructose, as a model compounds, can be used for the quantification of the carbohydrates in different samples by taking a photography of the μ PAD using a digital camera or a smartphone under UV LED lighting. In view of the operation simplicity from the synthesis of SNDs in this assay, with this method it is possible to monitor human glucose levels in biological samples such as serum and urine. Additionally, the proposed assay results suitable to estimate total sugar content in soft drinks. Thus, the results show that the proposed device is affordable, sensitive, quick and robust, portable, simple to use and green-friendly for the use of fluorescence tools in the point of care testing.

2. Experimental

2.2. Reagents and materials

Glucose, galactose, mannose, sucrose, fructose, maltose, trehalose, serine, histidine, lysine, arginine, asparagine, uric acid, urea, sodium hydroxide, sodium chloride, potassium chloride, calcium chloride, magnesium chloride, disodium hydrogen phosphate, sodium sulfate, (3-aminopropyl) triethoxysilane (APTS), Tris-HCl were from Sigma Aldrich (Madrid, Spain). All reagents used were of analytical-reagent-grade unless stated otherwise. Kapton[®] HN polyimide films with a thickness of 125 μ m was purchased from DuPont[™] (Constantine, MI, USA). Conductive silver/silver chloride (Ag/AgCl) ink from Loctite (Henkel, Germany). Whatman grade 1 chromatography paper from Sigma-Aldrich was used to manufacture the μ PAD. All aqueous solutions were made using purified water (18.2 M Ω ·cm resistance) was obtained from a Milli-RO 12 plus Milli-Q station (Millipore, Bedford, MA, USA).

2.2. Instruments and software

The fluorescence intensity of SNDs was measured with a Huawei Mate 10 lite smartphone (Huawei Technologies Co. Ltd., Shenzhen, China) after illumination with an UV LED. Custom made Android app was used to turn fluorescence intensity into colour and to analyse the region of interest (ROI) of the image. The analytical devices were fabricated on paper using a craft-cutting technique as a cost-efficient, simple and reproducible process using a 12 W CO₂ laser engraver (Rayjet, Barcelona, Spain).

The temperature response of the heater was also measured by applying voltage steps with Precision Source/Measurement Unit B2902 (Keysight Technologies, USA) while measuring temperature with IR camera Fluke TiS75 (Fluke Corporation, USA).

Fluorescence spectrum was collected using a Varian Cary Eclipse luminescence spectrometer (Varian Ibérica, Madrid, Spain). Absorbance spectrum was obtained using a Hewlett Packard diode array spectrophotometer (model 8453; Norwalk, CT, USA). Fourier-transform infrared (FT-IR) spectra were obtained using a Bruker Tensor 27 spectrometer under Attenuated Total Reflection (ATR) configuration with spectral resolution of 2 cm⁻¹ by accumulating 25 scans in the 4000–500 cm⁻¹ range. To investigate the size of SNDs, dynamic light scattering (DLS) assay was performed and Zeta potential measurements of SNDs in solutions at different pH values were measured by a Malvern zetasizer. The chemical composition of SNDs synthesized on paper (Si, C, O and N) was analyzed by X-ray photoelectron spectroscopy (XPS). The XPS spectra measurements were performed by Kratos Axis ultra-DLD. Also, by energy dispersive X-ray spectroscopy (EDX) measurements, the chemical composition of SNDs was contrasted. In addition, the distribution and compositional zonation of chemical elements in the paper was elucidated by an element mapping performed by energy-dispersive X-ray spectroscopy (EDS). SEM images were recorded with a QuenScan 650F FEI[®] electronic microscope together with an Everhart-Thornley detector 8ETD. Raman spectra were acquired with a JASCO 108 NRS-5100 dispersive micro-Raman spectrometer (from JASCO, Inc., Tokyo, Japan). All these studies were done at the Centre for Scientific Instrumentation (University of Granada).

2.3. Electronic device design

A device for temperature control has been developed. This device must be able to measure and change the temperature of the heater and communicate with a smartphone that acts as user interface. PSoC4 (Cypress Semiconductors, USA), has been selected for this purpose as it has Bluetooth 4.0 capabilities and analog and digital reconfigurable capabilities. Thanks to this interface, the user can use the smartphone to enable or disable the heat in the device and select the temperature of the heater when it is active. Also, the actual temperature of the heater is communicated to the user through this interface.

To supply power to the heater a current controlled DC/DC converter is employed. This device is controlled by a PWM generated by the PSoC4 which calculates the duty depending on the temperature measurement which is obtained from an IR thermopile sensor. The power can be supplied from two sources, a micro-USB connector or a Li-ion battery of 680 mAh which can supply the system for 13.6 hours. The micro-USB connector permits the use of any USB device or even an external battery for extended working time.

The electronics are integrated in a rigid-flex PCB of 22.50x32.49 mm as the one shown in the Figure 1A. The rigid-flex PCB allows the integration of the temperature sensor in the housing to measure the heater temperature just over it. The heater is connected through two pads in the bottom layer. To ensure a good contact, the housing press over these pads fixing the heater at the same time.

Temperature sensor is the thermopile sensor TSD305-1C55, which allows noncontact temperature sensing and I2C connection with the microcontroller. This sensor is connected through a flexible strip to place it over the heater as shown in Figure 1B. Figure 1C shows the aspect of the housing created in 3D to encapsulate the system, a window is open in this case to illuminate μ PAD and measure fluorescence intensity. To be able to measure fluorescence, the case has been designed to use a smartphone at a correct focus distance.

Finally, the PSoC4 can control a UV LED to excite the μ PAD. The LED employed is the EOLD-365-525 (OSA Opto Light, Berlin, Germany) which emits at $\lambda=365\text{nm}$.

Thanks to this feature and the design of the case, is possible to measure the sample with the device developed using a smartphone (Figure 1D).

2.4. Fabrication of the LIG heater

Heaters were fabricated using Kapton® HN (DuPont™) polyimide films with a thickness of 125 µm as raw material. A CO₂ laser was used to ablate this polyimide and to obtain conductive patterns. The laser employed was a 12W CO₂ laser engraver with a fixed wavelength of 10.6 µm (Rayjet, Barcelona, Spain). The laser was regulated at 20% of its maximum power and a 10% of its maximum speed, which means a power of 2.4 W and a speed of 0.15 m·s⁻¹. The substrate was placed at 5.08 cm from the laser head, allowing spatial resolution of 25 µm. With these parameters, it is possible to obtain LIG films with a sheet resistance of 90 Ω·sq⁻¹, while avoiding permanent deformations on the substrate. The sheet resistances were measured with B2901A Keysight source measurement unit (SMU) in a four-point measure configuration [35].

2.5. µPAD preparation

The µPADs were produced in a paper sheet using standard laboratory filter paper (Whatman n° 1) by craft cutting technique [36]. The device as shown in Figure 1D, containing three separates areas, one for the sample, the second for transporting the sample and third for the synthesis of SNDs and determination of total carbohydrates.

2.6. Measurement procedure

The determination of total carbohydrates expressed such as index of glucose or fructose were performed under the optimized conditions. The device was prepared by drop casting of 1 µL 98% of APTS solution onto the detection area. After, 7.5 µL of different concentrations of glucose or fructose (ranging from 10 to 1000 µM) were dropped onto the sampling area. The carbohydrate solution goes through to the detection area by capillarity. Then, the detection area of the µPAD was heat at 80°C for 30 min to ensure complete reaction between APTS and carbohydrates to synthesize the SNDs (Figure 2).

For the analysis of SNDs fluorescence intensity, the μ PADs were placed under a UV LED at 365 nm wavelength using a homemade accessory designed and made by us, Figure 1C. This accessory avoids that the light from the LED interferes in the measurement of SNDs fluorescence intensity and incorporates the electronic setup. Thereby, the accessory has a hole of 4 mm diameter to let the measure of SNDs fluorescence on the detection area of the μ PAD with a smartphone. The smartphone camera was placed in front of the accessory with the μ PAD to take photography of the detection area where the SNDs have been synthesized after reacting with standards or real samples containing glucose and/or fructose. The setting conditions used to photograph the detection area were: ISO 500, shutter speed 1/13s, aperture value f/2.20 and focal length of 35 mm.

The images acquired were processed using the same application that controls the instrument temperature. The images first were converted to gray scale and then they are analysed. First, the ROI that contains the analytical information in the detection area of 4mm is determined analysing the fluorescence intensity. Then, the software transformed each ROI into the gray scale space as the average of R, G and B coordinates from RGB (Red, Green, Blue) color space and this value was denoted by gray scale. Thus, an average of the gray scale coordinate from the pixels considered was calculated and used for the carbohydrates determination.

2.7. Treatment of real samples

To evaluate the feasibility of the developed μ PAD, the proposed method was applied to the determination of glucose in urine and serum, and the total carbohydrates content (glucose and fructose) in juices and teas samples. The urine samples were obtained from healthy volunteers. For glucose analysis in serum samples, artificial human serum was prepared according to the following composition: 137.5 mM NaCl, 4.2 mM NaHCO₃, 3 mM KCl, 0.5 mM Na₂HPO₄, 0.5 mM MgCl₂, 2.64 mM CaCl₂ and 0.5 mM Na₂SO₄. The pH value of the artificial serum samples were adjusted at 7.4 [37].

For the determination of glucose in serum and urine samples, these samples were spiked with a fixed glucose standard solution. After that, the samples were filtered through 0.22 μ m filter and were diluted 1:10 ratio in purified water.

Also, four different soft-drinks were purchased in local markets: pineapple juice, orange juice, tomato juice, black tea and green tea were also used to validate the sensor response. The samples were shaken before opening, diluted 1:1000 with purified water and filtered by a 0.22 μm pore diameter filter.

3. Results and discussion

3.2. Heater characterization

LIG heater was obtained from ablation of KaptonTM polyimide. As seen in Figure S1A the heaters have a dimension of 10x15 mm with two contacts of Ag/Cl ink, keeping a heating surface of around 10x10 mm. The heaters was characterized physically and electrically to determine its composition and behaviour. To confirm the graphene nature of the material obtained, Raman spectroscopy was employed, whose results are shown in Figure S1B. As shown, the spectrum is composed by 4 peaks (D, G, 2D and D+G). The G (1570 cm^{-1}) peak is related to the vibration of sp² pairs of atoms, whereas the D (1341 cm^{-1}) peak is associated to defects in the crystalline structure [38]. The 2D (2680 cm^{-1}) peak, characteristic of graphene layers, is the result of second order resonant process. G+D peak also accounts for defects in the structure. The coexistence of D and 2D peaks demonstrate that the structure differs of a monolayer graphene [39]. Moreover, the structure has several defects in the crystalline structure, confirmed by an ID/IG ratio close to 1, and it is composed by several layers of graphene, explained by the ratio I_{2D}/IG. The results show that the obtained material is derived from graphene, so it has some electrical conductivity. In Figure S1C and Figure S1D, SEM images of this heater are shown. As can be appreciated in the edge, laser changes the material for a uniform material with smooth surface to a porous irregular material. In detailed image this porosity can be appreciated more clearly.

The temperature response of the heater was also measured by applying voltage steps with Precision Source/Measurement Unit B2902 while measuring temperature with IR camera Fluke TiS75 Figure S2A. As can be seen in Figure S2B, the setting time is around 7 seconds. Power density needed for each temperature is shown in Figure S2C, it varies from 0 to $1.4\text{ W}\cdot\text{cm}^{-2}$ for temperatures from ambient to 300°C. Temperature vs voltage applied to the heater is shown in Figure S2D.

3.3. Characterization of SNDs

Silicon nanodots were synthesized in the detection area of the μ PAD through the reaction between APTS and glucose using a LIG heater. The nanoparticles were obtained after 30 min heating at 80°C, as indicated the results of XPS analysis (Figure S3). Figure S3A presents five peaks at 101.2, 152.3, 284.4, 397.5 and 531.2 eV corresponding to Si 2p, Si 2s, C 1s, N 1s and O 1s, respectively. The high-resolution scans show four different chemical bonds for C 1s at 283.2, 284.3, 285.6 and 286.8 eV corresponding to the presence of C-Si, C-C/C=C, C-N and C-OH/C-O-C groups, as shown in Figure S3B. The high-resolution N 1s spectrum present three different peaks at 398.4, 399.2 and 400.5 eV which were associated with N-Si, C-N-C and C-N=C groups (Figure S3C). Three peaks at 528.2, 531.2 and 533.5 eV were attributed to Si-O, and C-O in the high-resolution XPS spectrum of O 1s (Figure S3D). The Si 2p spectrum presents three peaks at 100.1, 101.2 and 102.2 eV, which were associated with Si-C, Si-N and Si-O groups, respectively (Figure S3E).

FT-IR spectrum over the range 500-4000 cm^{-1} confirms the presence of various chemical bonds in SNDs as shown in Figure S4A. The FT-IR spectra of the μ PAD containing the synthesized SNDs were recorded, which several distinct absorption peaks in the range of 1000-3500 cm^{-1} . The characteristic peaks of the stretching vibration of Si-C and Si-O were showed at 1250 and 1050 cm^{-1} respectively. The strong peaks at 1500 and 3300 cm^{-1} are assigned to the N-H bending vibration. As conclusion, it is indicated the presence of SNDs on the paper surface [14], [40].

In order to know the size of synthesized SNDs, transmission electron microscopy (TEM) and DLS assays were performed. As shown in Figure S4B the diameters of SNDs ranged from 1 to 4 nm with uniform dispersion. This results is consistent with that from DLS. In this case, the SNDs were synthesized on the μ PAD under optimal condition using nine different μ PADs. After that, the μ PADs were immersed on purified water to drag the synthesized SNDs. As shown in Figure S4C the diameters of SNDs ranged from 2 to 6 nm with uniform dispersion. This results are consistent with the values reported in the bibliography [41]. In addition, zeta potential measurements of SNDs in solutions at three different pH values 1, 7 and 12 were measured by a Malvern Zetasizer. Data were acquired in the phase analysis light scattering mode following solution equilibration at 25°C. The changes of zeta potential values measured using for

synthesized SNDs on paper and dissolved in purified water was carried out. It was observed that at pH 1 the zeta potential of SNDs was +18.9 mV. However, when the pH was raised to 7 or 12 the zeta potential was reduced to 1.2 mV or -4.6 mV, respectively due to the reduction in the number of protonated amine groups.

On the other hand, the optical properties of SNDs were investigated, UV-Vis spectra of SNDs was collected by using Agilent Cary UV-Vis spectrometer. Figure S4D is the UV-vis absorption spectrum of SNDs synthesized on the μ PAD and dragged on purified water. The spectrum exhibits a strong absorption peak centered at 330 nm. Fluorescence spectra of SNDs were measured from 300 to 400 nm. As shown in Figure S4E the maximum emission peak at 475 nm under the excitation of 410 nm.

3.4. Optimization of method

The chemical conditions under which the carbohydrates determination is carried out are the result of balancing the conditions needed for both the recognition and transduction steps therefore the following parameters were optimized: concentration of APTS, pH of reaction, temperature, reaction time and volume of sample. The following experimental conditions were found to give best results: (A) the concentration selected as optimum for APTS was $0.88 \text{ mmol}\cdot\text{mm}^{-2}$; (B) the SNDs present a strong stability at pH range between 2 and 12 (C) the temperature selected as optimum for the synthesis of SNDs was $80 \text{ }^\circ\text{C}$; (D) the reaction time required to complete the assay is 30 min and (E) the volume of sample selected as optimum $7.5 \text{ }\mu\text{L}$ of glucose. Respective data are given in the Electronic Supporting Material Figure S5.

3.5. Calibration and analytical parameters

The developed μ PAD is based on the synthesis of silicon nanodots prepared from APTS and carbohydrates by heating with a flexible, portable and reusable LIG heater. SNDs synthesized by redox reaction between carbohydrates, which acts as reducer, and APTS exhibited high blue fluorescence with an emission peak wavelength of 475 nm. The fluorescence intensity of SNDs increases when the concentration of carbohydrates increases. This increase of fluorescence can be quantified by correlating the

fluorescence intensity measured as grey intensity of the μ PAD with the total concentration of carbohydrates present in the sample (Figure 3). For this determination, photography of the μ PAD was carried out after reaction with glucose or fructose using a smartphone Figure 3. The analytical functions were obtained by means of a calibration set composed of 12 standards with 3 replicates each obtained with a new μ PAD each time between 10 and 200 μ M for glucose and 10 to 100 μ M for fructose. The performance analytical characteristics of the μ PAD developed are presented in Table 1. The limit of detection (LOD) was obtained using the standard criteria $LOD = 3\sigma/\text{slope}$ where σ is the standard deviation of the blank, which was determined from 12 blanks (relative standard deviation (RSD) 1.13). With this criterion, the value of the LOD was 0.80 μ M for glucose and 0.51 μ M for fructose and the limit of quantification (LOQ) 2.68 μ M and 1.55 μ M for glucose and fructose, respectively. The repeatability as RSD, obtained using 8 different μ PADs at 40 μ M and 100 μ M glucose, was 2.64% and 1.84%, respectively. It is an acceptable precision considering the measuring system used.

3.6. Study and evaluation of potential interferences

The effect of different compounds commonly present in biological samples such as serine, histidine, lysine, arginine, asparagine, uric acid, urea, NaCl, KCl, CaCl₂, MgCl₂, Na₂HPO₄, Na₂SO₄ and monosaccharides and disaccharides such as galactose, fructose, sucrose, maltose, trehalose and mannose was evaluated. The data shows that the SNDs exhibited excellent properties as a fluorescence probe for carbohydrates over other amino acids and inorganic salts. The fluorescence intensity increases when carbohydrates such as glucose, fructose, galactose, sucrose, maltose, trehalose and mannose were present on the sample (Figure 4). The response of this μ PAD to both reducing and non-reducing carbohydrates is explained by the experimental condition, high temperature and acidic medium can produce the hydrolysis of disaccharides present in the samples to reducing glucose and fructose. Therefore, this method can be applied to determination of total carbohydrates expressed such as an index of glucose without significant interferences [14] in biological samples (serum and urine). Anyway it is necessary remember that the concentration of carbohydrates in normal human serum and urine is at least ten times lower than that of glucose.

3.7. Analysis of real samples

Glucose plays an important role in the life system. For example, to know the glucose concentration is essential for the care of people with diabetes. For that, the human serum and urine samples were often used as test samples to investigate the glucose concentration levels. Thus, serum samples from healthy human have a normal content of glucose between 3.9 and 6.1 mmol·L⁻¹ [42]. On the other hand, the normal fasting urine glucose level in the healthy human urine are around 0.8 mmol·L⁻¹ [43]. In this way, in order to evaluate the feasibility of practical application of the developed μ PAD in the analysis of biological samples such as urine and serum, the recovery experiments of standard addition were carried out. The detection results for glucose are shown in Table 2. For urine samples, the recovery experiment was carried out by spiking of 10, 20 and 30 μ M of standard glucose. Also, the artificial serum samples were spiked of 10, 20, 30 and 50 μ M of standard glucose solutions. Thereby, the recoveries obtained for urine and serum samples are in the range of 99.23 – 109.70 % and 103.46 – 113.80%, respectively. The results demonstrate that the method proposed in this work can be used for determination of glucose in real samples obtaining good recovery percentage.

On the other hand, the determination of carbohydrates content in foodstuff such as soft-drinks, mainly juices and teas, which have a high level of carbohydrates content, is an important issue in food quality control [44]. In this way, we have evaluated the amount of carbohydrates present in three different juices and two teas. These samples content three different types of sugar mainly: sucrose, fructose and glucose. Thereby, the acidic pH of these drinks generally leads to the slow conversion of sucrose into its two constituent carbohydrates: glucose and fructose, whereas in natural samples, glucose and fructose naturally results the most representative carbohydrates [44]. In this way, we have determined the global content of carbohydrate as an index of glucose presents in these samples. The detection results from the previous method are basically consistent with the known contents. The values reported are the average of the measurements performed using 9 different sensors. The results found are satisfactory when it compared with the labelled of the drinks such as shown in the Table 3.

Conclusion

In summary, a sensitive, highly robust and cost-efficient μ PAD for determination of total carbohydrates has been designed. The device is based on the synthesis of fluorescent silicon nanodots by heating the μ PAD with APTS and carbohydrates, using glucose and fructose as a model, using a flexible, portable and reusable LIG heater. The recognition is based on a redox reaction between APTS and carbohydrates, which acts such as reducer. The resulting fluorescence intensity allows the rapid screening of carbohydrate by the use of a UV LED and a smartphone. We expect that this method may open up a new path in developing low-cost and ecofriendly method for biological diagnostics application.

Acknowledgements

This work was founded by Spanish “Ministerio de Economía y Competitividad” (Projects PID2019-103938RB-I00 and CTQ2017-86125-P) and Junta de Andalucía (Projects B-FQM-243-UGR18 and P18-RT-2961). The projects were partially supported by European Regional Development Funds (ERDF).

References

- [1] A. W. Martinez, S. T. Phillips, M. J. Butte, and G. M. Whitesides, “Patterned paper as a platform for inexpensive, low-volume, portable bioassays.,” *Angew. Chem. Int. Ed. Engl.*, vol. 46, no. 8, pp. 1318–1320, 2007.
- [2] D. Mark, S. Haeblerle, G. Roth, F. Von Stetten, and R. Zengerle, “Microfluidic lab-on-a-chip platforms: Requirements, characteristics and applications,” *Chem. Soc. Rev.*, vol. 39, no. 3, pp. 1153–1182, 2010.
- [3] Y. Xia, J. Si, and Z. Li, “Fabrication techniques for microfluidic paper-based analytical devices and their applications for biological testing: A review.,” *Biosens. Bioelectron.*, vol. 77, pp. 774–789, Mar. 2016.
- [4] J. Hu *et al.*, “Advances in paper-based point-of-care diagnostics,” *Biosens. Bioelectron.*, vol. 54, pp. 585–597, 2014.
- [5] A. K. Yetisen, M. S. Akram, and C. R. Lowe, “Paper-based microfluidic point-

- of-care diagnostic devices,” *Lab Chip*, vol. 13, no. 12, pp. 2210–2251, 2013.
- [6] D. Mark, S. Haeberle, G. Roth, F. von Stetten, and R. Zengerle, “Microfluidic lab-on-a-chip platforms: requirements, characteristics and applications,” *Chem. Soc. Rev.*, vol. 39, no. 3, pp. 1153–1182, 2010.
- [7] V. Gubala, L. F. Harris, A. J. Ricco, M. X. Tan, and D. E. Williams, “Point of Care Diagnostics: Status and Future,” *Anal. Chem.*, vol. 84, no. 2, pp. 487–515, Jan. 2012.
- [8] L. Shen, J. A. Hagen, and I. Papautsky, “Point-of-care colorimetric detection with a smartphone,” *Lab Chip*, vol. 12, no. 21, pp. 4240–4243, 2012.
- [9] B. M. Jayawardane, I. D. McKelvie, and S. D. Kolev, “Development of a Gas-Diffusion Microfluidic Paper-Based Analytical Device (μ PAD) for the Determination of Ammonia in Wastewater Samples,” *Anal. Chem.*, vol. 87, no. 9, pp. 4621–4626, May 2015.
- [10] D. M. Cate, J. A. Adkins, J. Mettakoonpitak, and C. S. Henry, “Recent Developments in Paper-Based Microfluidic Devices,” *Anal. Chem.*, vol. 87, no. 1, pp. 19–41, Jan. 2015.
- [11] L. Syedmoradi, M. Daneshpour, M. Alvandipour, F. A. Gomez, H. Hajghassem, and K. Omidfar, “Point of care testing: The impact of nanotechnology,” *Biosens. Bioelectron.*, vol. 87, pp. 373–387, 2017.
- [12] C. Dincer *et al.*, “Disposable Sensors in Diagnostics, Food, and Environmental Monitoring,” *Adv. Mater.*, vol. 31, no. 30, 2019.
- [13] B. Sharma, S. Tanwar, and T. Sen, “One Pot Green Synthesis of Si Quantum Dots and Catalytic Au Nanoparticle-Si Quantum Dot Nanocomposite,” *ACS Sustain. Chem. Eng.*, vol. 7, no. 3, pp. 3309–3318, 2019.
- [14] Q. Cai, H. Meng, Y. Liu, and Z. Li, “Fluorometric determination of glucose based on a redox reaction between glucose and aminopropyltriethoxysilane and in-situ formation of blue-green emitting silicon nanodots,” *Microchim. Acta*, vol. 186, no. 2, 2019.
- [15] J. G. Croissant, Y. Fatieiev, A. Almalik, and N. M. Khashab, “Mesoporous Silica and Organosilica Nanoparticles: Physical Chemistry, Biosafety, Delivery

- Strategies, and Biomedical Applications,” *Adv. Healthc. Mater.*, vol. 7, no. 4, p. 1700831, Feb. 2018.
- [16] S. Chandra, Y. Masuda, N. Shirahata, and F. M. Winnik, “Transition-Metal-Doped NIR-Emitting Silicon Nanocrystals,” *Angew. Chemie Int. Ed.*, vol. 56, no. 22, pp. 6157–6160, May 2017.
- [17] J. G. Croissant, X. Cattoën, J.-O. Durand, M. Wong Chi Man, and N. M. Khashab, “Organosilica hybrid nanomaterials with a high organic content: syntheses and applications of silsesquioxanes,” *Nanoscale*, vol. 8, no. 48, pp. 19945–19972, 2016.
- [18] B. F. P. McVey and R. D. Tilley, “Solution Synthesis, Optical Properties, and Bioimaging Applications of Silicon Nanocrystals,” *Acc. Chem. Res.*, vol. 47, no. 10, pp. 3045–3051, Oct. 2014.
- [19] T. Bose, Sandeep Ganayee, Mohd. Azhardin Mondal, Biswajit Baidya, Avijit Chennu, Sudhakar Mohanty, Jyoti Sarita Pradeep, “Synthesis of Silicon Nanoparticles from Rice Husk and their Use as Sustainable Fluorophores for White Light Emission,” *ACS Sustain. Chem. Eng.*, vol. 6, no. 5, pp. 6203–6210, May 2018.
- [20] J. Zhang and S.-H. Yu, “Highly photoluminescent silicon nanocrystals for rapid, label-free and recyclable detection of mercuric ions,” *Nanoscale*, vol. 6, Mar. 2014.
- [21] Y. Zhong, Yiling Sun, Xiaotian Wang, Siyi Peng, Fei Bao, Feng Su, Yuanyuan Li, Youyong Lee, Shuit-Tong He, “Facile, Large-Quantity Synthesis of Stable, Tunable-Color Silicon Nanoparticles and Their Application for Long-Term Cellular Imaging,” *ACS Nano*, vol. 9, no. 6, pp. 5958–5967, Jun. 2015.
- [22] L. Mohapatra, Pratyasha Mendivelso-Perez, Deyny Bobbitt, Jonathan M. Shaw, Santosh Yuan, Bin Tian, Xinchun Smith, Emily A. Cademartiri, “Large-Scale Synthesis of Colloidal Si Nanocrystals and Their Helium Plasma Processing into Spin-On, Carbon-Free Nanocrystalline Si Films,” *ACS Appl. Mater. Interfaces*, vol. 10, no. 24, pp. 20740–20747, Jun. 2018.
- [23] G. A. Mastronardi, Melanie L. Hennrich, Frank Henderson, Eric J. Maier-Flaig, Florian Blum, Carolin Reichenbach, Judith Lemmer, Uli Kübel, Christian Wang,

- Di Kappes, Manfred M. Ozin, "Preparation of Monodisperse Silicon Nanocrystals Using Density Gradient Ultracentrifugation", *J. Am. Chem. Soc.*, vol. 133, no. 31, pp. 11928–11931, Aug. 2011.
- [24] X. Zhai, B. Song, B. Chu, Y. Su, H. Wang, and Y. He, "Highly fluorescent, photostable, and biocompatible silicon theranostic nanoprobe against *Staphylococcus aureus* infections," *Nano Res.*, vol. 11, no. 12, pp. 6417–6427, Dec. 2018.
- [25] Y. He, Yao Zhong, Yiling Peng, Fei Wei, Xinpan Su and S.-T. Lu, Yimei Su, Shao Gu, Wei Liao, Liangsheng Lee, "One-Pot Microwave Synthesis of Water-Dispersible, Ultraphoto- and pH-Stable, and Highly Fluorescent Silicon Quantum Dots," *J. Am. Chem. Soc.*, vol. 133, no. 36, pp. 14192–14195, Sep. 2011.
- [26] X. Zhong, Yiling Peng, Fei Bao, Feng Wang, Siyi Ji and Y. Yang, Liu Su, Yuanyuan Lee, Shuit-Tong He, "Large-Scale Aqueous Synthesis of Fluorescent and Biocompatible Silicon Nanoparticles and Their Use as Highly Photostable Biological Probes," *J. Am. Chem. Soc.*, vol. 135, no. 22, pp. 8350–8356, Jun. 2013.
- [27] Y. Zhong, Yiling Sun, Xiaotian Wang, Siyi Peng, Fei Bao, Feng Su, Yuanyuan Li, Youyong Lee, Shuit-Tong He, "Facile, Large-Quantity Synthesis of Stable, Tunable-Color Silicon Nanoparticles and Their Application for Long-Term Cellular Imaging," *ACS Nano*, vol. 9, no. 6, pp. 5958–5967, Jun. 2015.
- [28] Y. Zhong, Yiling Peng, Fei Wei, Xinpan Zhou, Yanfeng Wang, Jie Jiang, Xiangxu Su, Yuanyuan Su, Shao Lee, Shuit-Tong He, "Microwave-Assisted Synthesis of Biofunctional and Fluorescent Silicon Nanoparticles Using Proteins as Hydrophilic Ligands," *Angew. Chemie Int. Ed.*, vol. 51, no. 34, pp. 8485–8489, Aug. 2012.
- [29] G. Chen, Haoyu Wu, Li Wan, Yuqi Huang, Lulu Li, Ningxing Chen, Jinyang Lai, "One-step rapid synthesis of fluorescent silicon nanodots for a hydrogen peroxide-related sensitive and versatile assay based on the inner filter effect," *Analyst*, vol. 144, no. 13, pp. 4006–4012, 2019.
- [30] C. Li *et al.*, "Flexible graphene electrothermal films made from electrochemically exfoliated graphite," *J. Mater. Sci.*, vol. 51, no. 2, pp. 1043–1051, Jan. 2016.

- [31] S. Xie, T. Li, Z. Xu, Y. Wang, X. Liu, and W. Guo, "A high-response transparent heater based on a CuS nanosheet film with superior mechanical flexibility and chemical stability," *Nanoscale*, vol. 10, no. 14, pp. 6531–6538, 2018.
- [32] K. Handique, "Microfluidic cartridge and method of making same," US8709787B2, 2004.
- [33] A. C. Catto *et al.*, "An easy method of preparing ozone gas sensors based on ZnO nanorods," *RSC Adv.*, vol. 5, no. 25, pp. 19528–19533, 2015.
- [34] N. Romero, Francisco J. Rivadeneyra, Almudena Ortiz-Gomez, Inmaculada Salinas, Alfonso Godoy, Andrés Morales, Diego P. Rodriguez, "Inexpensive Graphene Oxide Heaters Lithographed by Laser," *Nanomaterials*, vol. 9, no. 9, p. 1184, Aug. 2019.
- [35] M. R. Bobinger *et al.*, "Flexible and robust laser-induced graphene heaters photothermally scribed on bare polyimide substrates," *Carbon N. Y.*, vol. 144, pp. 116–126, Apr. 2019.
- [36] I. Ortiz-Gomez *et al.*, "A vinyl sulfone clicked carbon dot-engineered microfluidic paper-based analytical device for fluorometric determination of biothiols," *Microchim. Acta*, vol. 187, no. 7, p. 421, 2020.
- [37] M. Basiaga, Z. Paszenda, W. Walke, and J. Karasiński Paweł and Marciniak, "Electrochemical Impedance Spectroscopy and Corrosion Resistance of SiO₂ Coated CpTi and Ti-6Al-7Nb Alloy," in *Information Technologies in Biomedicine, Volume 4*, 2014, pp. 411–420.
- [38] F. Tuinstra and J. L. Koenig, "Raman Spectrum of Graphite," *J. Chem. Phys.*, vol. 53, no. 3, pp. 1126–1130, Aug. 1970.
- [39] A. C. Ferrari *et al.*, "Raman Spectrum of Graphene and Graphene Layers," *Phys. Rev. Lett.*, vol. 97, no. 18, p. 187401, Oct. 2006.
- [40] H. Chen *et al.*, "One-step rapid synthesis of fluorescent silicon nanodots for a hydrogen peroxide-related sensitive and versatile assay based on the inner filter effect," *Analyst*, vol. 144, no. 13, pp. 4006–4012, 2019.
- [41] B. Sharma and S. Tanwar, "One Pot Green Synthesis of Si Quantum Dots and Catalytic Au Nanoparticle-Si Quantum Dot Nanocomposite," *ACS Sustain.*

Chem. Eng., vol. 7, Jan. 2019.

- [42] Y. Qi, Y. Chen, J. He, and X. Gao, “Highly sensitive and simple colorimetric assay of hydrogen peroxide and glucose in human serum via the smart synergistic catalytic mechanism,” *Spectrochim. Acta Part A Mol. Biomol. Spectrosc.*, vol. 234, p. 118233, 2020.
- [43] D. O. F. Kidney, “Laboratory Assessment of Kidney Disease,” *Pocket Companion to Brenner Rector’s Kidney*, pp. 21–41, 2011.
- [44] F. Della Pelle, A. Scroccarello, S. Scarano, and D. Compagnone, “Silver nanoparticles-based plasmonic assay for the determination of sugar content in food matrices,” *Anal. Chim. Acta*, vol. 1051, pp. 129–137, 2019.

Table 1. Analytical characteristics of μ PAD for glucose or fructose determination.

Analytical parameter	Values for glucose	Values for fructose
Measurement range, μM	2.68 – 200.00	1.55 – 100.00
Slope	0.51	0.79
Intercept	20.56	6.82
LOD, μM	0.80	0.51
LOQ, μM	2.68	1.55
Precision, % 40 μM	2.64	-
Precision, % 100 μM	1.84	-

Table 2. Determination of glucose in human urine samples.

Sample	Found, μM	Added, μM	Total found, μM	Recovery, %
Urine 1	25.56	10.00	36.53	109.70
		20.00	46.07	102.55
		30.00	55.33	99.23
Urine 2	30.90	10.00	41.49	105.90
		20.00	53.66	113.80
		30.00	61.94	103.46
Serum	-	10.00	10.74	107.40
		20.00	19.47	97.33
		30.00	30.27	100.92
		50.00	50.00	99.99

Table 3. Determination of total carbohydrates in commercial juices and teas (n = 9).

Samples	Labelled g·mL⁻¹	Found g·mL⁻¹
Pineapple juice	0.026	0.02 ± 0.003
Orange juice	0.102	0.09 ± 0.011
Tomato juice	0.035	0.03 ± 0.006
Black tea	0.045	0.04 ± 0.003
Green tea	0.082	0.07 ± 0.002

Figure captions

Figure 1. Hardware characteristics. (A) Board dimensions and distribution; (B) Folder state of the board inside the housing; (C) Housing made for the board; (D) Microfluidic paper-based analytical device for determination total carbohydrates with synthesized SNDs; (E) Portable housing accomplished to the smartphone.

Figure 2. Schematic illustration of SNDs synthesis from APTS and carbohydrate.

Figure 3. Calibration curve for (A) glucose and (B) fructose. Conditions: 1 μL APTS; heating at 80°C for 30 min; 7.5 μL of glucose or fructose solutions; $\lambda_{\text{exc}} = 365$ nm. Data points are the mean of 3 assays

Figure 4. Response of different interferences and carbohydrates. Conditions: 1 μL APTS; heating at 80°C for 30 min; 7.5 μL of interference solutions 250 μM ; $\lambda_{\text{exc}} = 365$ nm. Data points are the mean of 3 assays.

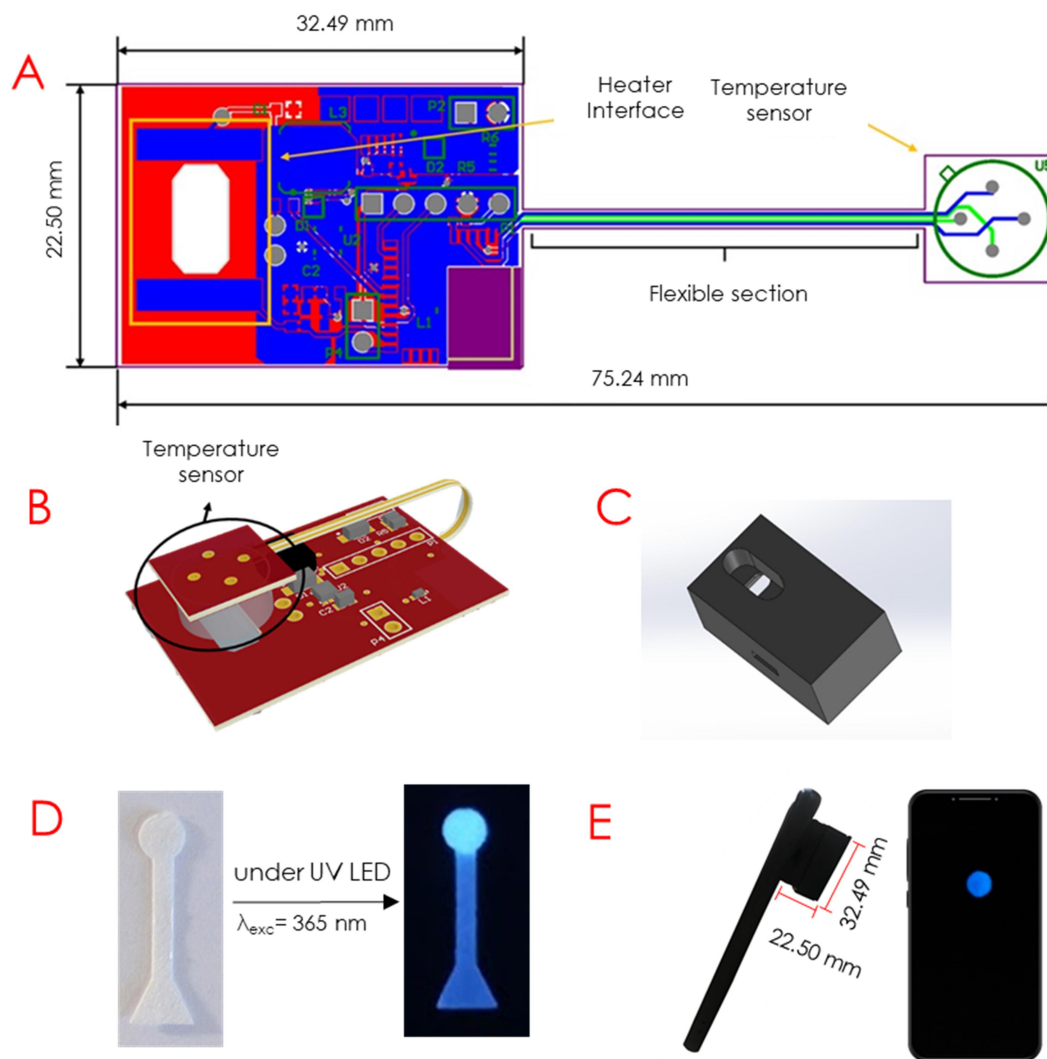


Figure 1. Hardware characteristics. (A) Board dimensions and distribution; (B) Folder state of the board inside the housing; (C) Housing made for the board; (D) Microfluidic paper-based analytical device for determination total carbohydrates with synthesized SNDs; (E) Portable housing accomplished to the smartphone.

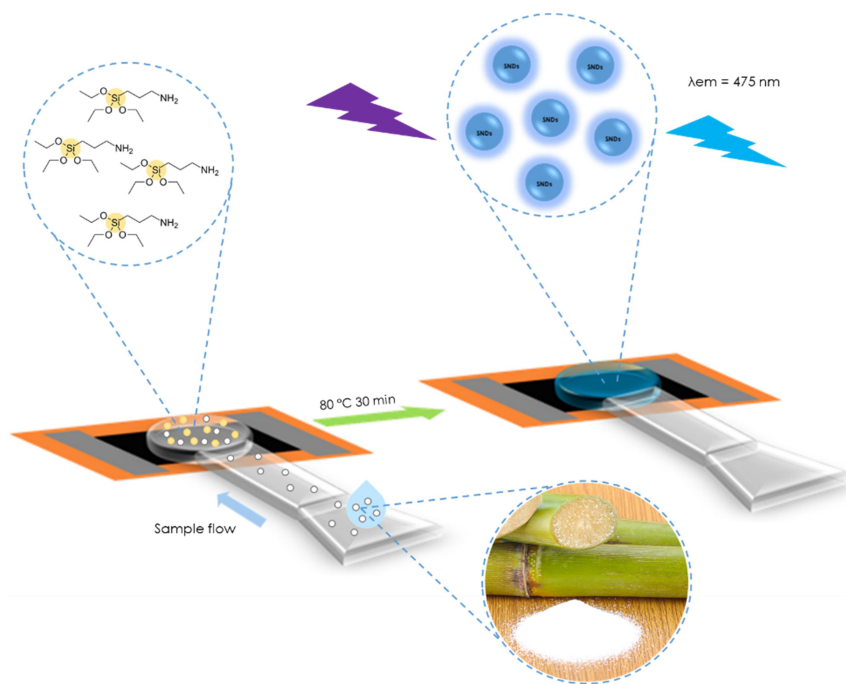


Figure 2. Schematic illustration of SNDs synthesis from APTS and carbohydrate.

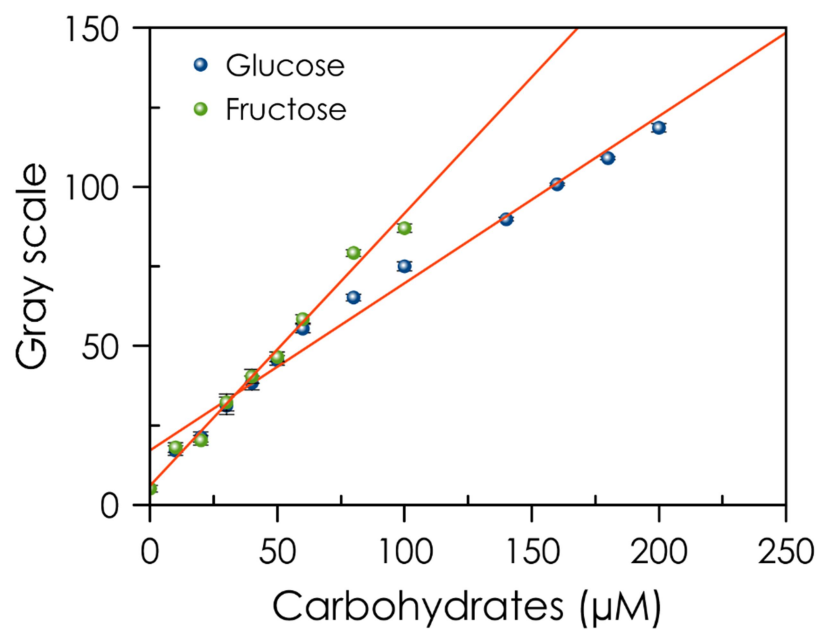


Figure 3. Calibration curve for (A) glucose and (B) fructose. Conditions: 1 µL APTS; heating at 80°C for 30 min; 7.5 µL of glucose or fructose solutions. Data points are the mean of 3 assays.

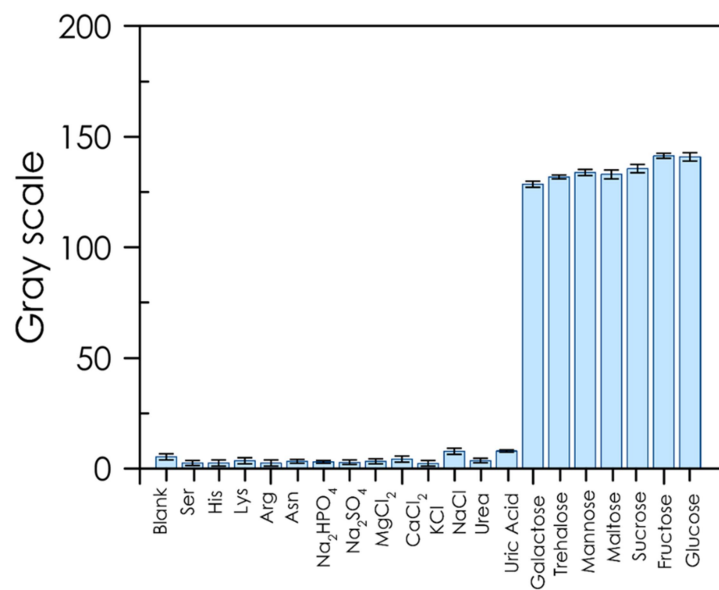


Figure 4. Response of different compounds and carbohydrates. Conditions: 1 μ L APTS; heating at 80°C for 30 min; 7.5 μ L of interference solutions 250 μ M.

Data points are the mean of 3 assays.

Author Biographies

Inmaculada Ortiz Gómez received the Major degree in Chemistry from the University of Granada (Granada, Spain) in 2015 and 2016, respectively, and the Master's degree in Research, development, control and innovation of medicines. Ph.D. in Analytical Chemistry (2020) at the University of Granada. Nowadays, she has a researcher contract in the ECSens Group, Department of Analytical Chemistry. Her research interests include the design and characterization of microfluidic capillary devices.

Víctor Toral-López received the B.Eng. degree in electronic engineering from the University of Granada, in 2017, and the M.Eng. degree in electronics engineering from the Polytechnic University of Madrid, in 2018. He is currently pursuing the Ph.D. degree with the Department of Electronics and Computer Technology, University of Granada. His current research interests include biomedical electronics, reconfigurable instrumentation, and flexible electronics.

Francisco J Maldonado received the B.Eng. with valedictorian mention in Telecommunication Engineering from the University of Granada (Spain) in 2016. In 2015, he joined the Department of Electronics and Computer Technology at the University of Granada as a Junior Researcher, and in 2017 became a PhD Candidate with a national predoctoral scholarship. His current research interests are related to 2D-materials-based sensors, flexible electronics and IoT embedded systems.

Ignacio de Orbe-Payá is currently Associate Professor of the Department of Analytical Chemistry at the University of Granada (Spain). His main areas of interest are the development of the sensing phases for multianalyte sensing using multivariate calibration methods for environmental, biomedical and food analysis.

Antonio García received the M.A.Sc. degree in electronic engineering, the M.Sc. degree in physics (majoring in electronics), and the Ph.D. degree in electronic engineering from the University of Granada, Granada, Spain, in 1995, 1997, and 1999, respectively. He was an Associate Professor with the Department of Computer Engineering, Universidad Autónoma de Madrid, Madrid, Spain, before joining the Department of Electronics and Computer Technology, University of Granada, where he actually serves as a Full Professor. He was also a Visiting Professor with the

Department of Electrical and Computer Engineering, FAMU-FSU College of Engineering, Tallahassee, FL, from August 2017 to January 2018. He has authored more than 130 technical papers in international journals and conferences. Dr. García is a CAS and SP Society Member. He received the National Award to the Best Academic Record for his M.A.Sc. degree. He serves as reviewer and a guest editor for several journals and has been part of the program committee for several international conferences on programmable logic.

Noel Rodríguez received the Electronics Engineer degree (B.Sc. + M.Eng.) from the University of Granada in 2004 obtaining the first national award of university education. In 2008, he received a double Ph.D. from the University of Granada and the National Polytechnic Institute of Grenoble (France) with the extraordinary award. He is a Tenured Professor of Electronics at the Department of Electronics and Computer Technology and co-founder of the Pervasive Electronics Advanced Research Laboratory (PEARL) at the University of Granada. His current research lines cover low-power energy conversion, electric mobility, non-conventional electronics, and new materials and devices for electronic applications. He has co-authored 15 international patents and more than 100 scientific contributions.

Luís Fermín Capitán-Vallvey Full Professor of Analytical Chemistry at the University of Granada, received his BSc in Chemistry (1973) and PhD in Chemistry (1986) from the Faculty of Sciences, University of Granada (Spain). In 1983, he founded the Solid Phase Spectrometry group (GSB) and in 2000, together with Prof. Palma López, the interdisciplinary group ECsens, which includes Chemists, Physicists and Electrical and Computer Engineers at the University of Granada. His current research interests are the design, development and fabrication of sensors and portable instrumentation for environmental, health and food analysis and monitoring. Recently is interested in printing chemical sensor and capillary-based microfluidic devices. His work has produced nearly 370 peer-reviewed scientific papers, 6 books, 25 book chapters and 6 patents.

Diego P. Morales received the M.A.Sc degree in Electronic Engineering and the Ph.D. degree in Electronic Engineering from the University of Granada (Granada, Spain) in 2001 and 2011, respectively. He was an Associate Professor at the Department of Computer Architecture and Electronics, University of Almería (Almería, Spain) before

joining the Department of Electronics and Computer Technology at the University of Granada, where he currently serves as an Associate Professor (tenure track). His current research is devoted to develop electronic applications for two imbricated areas, wearable and flexible electronic systems and processing for environmental and biomedical signals. In addition, understanding and handling power electronic systems for emerging areas are in his foreseeing research. He is cofounder of the Biochemistry and Electronics as Sensing Technologies research group (BEST research group).

Alfonso Salinas-Castillo (Granada, 1978) received the M.Sc.degree in Chemistry (2001) and Ph.D. in Analytical Chemistry (2005), both from the University of Granada and is currently Associate Professor of the Department of Analytical Chemistry. He is currently working at the ECsens Group, Department of Analytical Chemistry, University of Granada. His current research interest includes optical sensor and biosensor, luminescent nanoparticle and colorimetric sensor.